ELSEVIER

Computational Materials Science 29 (2004) 301–308

COMPUTATIONAL MATERIALS SCIENCE

www.elsevier.com/locate/commatsci

Simulation of polycrystalline structure with Voronoi diagram in Laguerre geometry based on random closed packing of spheres

Zhigang Fan, Yugong Wu *, Xuanhe Zhao, Yuzhu Lu

School of Electronic and Information Engineering, Tianjin University, Tianjin 300072, People's Republic of China

Received 25 February 2003; received in revised form 1 October 2003; accepted 9 October 2003

Abstract

A type of diagram is proposed as microstructure model of polycrystalline materials, Voronoi diagram in the Laguerre geometry based on random closed packing of spheres (RCP-LV diagram), and discussed in detail. The volumes of spheres are set to serve lognormal distribution, which is strongly inherited by distribution of cell volumes in the RCP-LV diagram. The geometrical and topological properties in the RCP-LV diagram and the Poisson–Voronoi diagram (PV diagram) are compared with those properties of real polycrystalline materials, and it is found that the lognormal distribution is a better approximation to the cell volume and face number distribution in the RCP-LV diagram than in the PV diagram. It is also shown clearly that coefficient of variance of cell volumes in the RCP-LV diagram is controlled by coefficient of variance of sphere volumes. This makes it easy to simulate polycrystalline microstructure with different dispersion of grain volumes. The RCP-LV diagram is probably superior to the PV diagram for the simulation of polycrystalline materials.
© 2003 Elsevier B.V. All rights reserved.

PACS: 7.05.T; 82.20.Wt; 81.40.−z

Keywords: Simulation; Microstructure; RCP-LV diagram; Voronoi diagram; Possion–Voronoi diagram; Volume distribution; Face number distribution; Grain growth

1. Introduction

Because polycrystalline material structure is composed of an enormous number of grains, its properties and performance are determined not only by characteristics of individual grains but also by the connectivity and interaction between them. In simulation of material properties, it is a key step to construct a model accurate enough to represent the microstructure of real material. During the past decades, several types of models has been used to simulate microstructure, among which the Poisson–Voronoi diagram (PV diagram) has been extensively used and studied by Meijering [1], Gilbert [2] and Kumar et al. [3]. The PV diagram is composed of an array of convex, space-filling and non-overlapping polyhedrons, which can be used to represent the grains of polycrystalline material. The polyhedrons of the PV diagram possess the properties that four edges share a vertex and three faces share an edge, which are also observed in real

* Corresponding author. Tel.: +86-22-2740-2372; fax: +86-22-2740-1471.

E-mail address: wuyugong@yahoo.com.cn (Y. Wu).

0927-0256/$ - see front matter © 2003 Elsevier B.V. All rights reserved.
doi:10.1016/j.commatsci.2003.10.006

material. However, some inadequate features of the PV diagram do exist in representation of real material: The average number of faces per polyhedron is 15.5355 in the PV diagram [3], beyond the range of 12–14, where the average number per grain in real material lies [4–9]; the polyhedron volumes are assumed to obey a gamma distribution in the PV diagram [3], but grain volumes usually have lognormal distribution in a real material [10,11]; moreover, real materials usually have a coefficient of variation (CV) of grain volumes, ranging from 1.09 to 2.13 [10], which is obviously greater than the invariant CV value of polyhedron volumes in the PV diagram (0.424) [3]. Therefore, it seems not adequate for the PV diagram with such a fixed CV value to accurately represent various real materials with quite different statistical characteristics.

In this paper, a model referred to as the RCP-LV diagram, which is probably better than the PV diagram in simulation of real material, is proposed. Construction of this model will be described in detail in Section 2; thereafter, in Section 3, the corresponding properties in the RCP-LV diagram and the PV diagram are discussed, vis-a-vis the geometrical and topological properties in real materials. Eventually, a conclusion is drawn that RCP-LV diagram is probably superior to the PV diagram for simulation of polycrystalline materials.

2. Modeling

The model proposed in this paper is referred to as the RCP-LV diagram, that is the Voronoi diagram in the Laguerre geometry based on random closed packing of spheres.

2.1. Voronoi diagram

The Voronoi diagram (VD) is constructed with a set of n separate points, $S = \{p_1, p_2, \ldots, p_n\}$. If the normal Euclidean distance between p_i and any other point q in the space is denoted as $d_E(p_i, q)$, a Voronoi cell (v-cell) corresponding to p_i is defined as

$$v_E(p_i) = \{p | p \in R^3,\ d_E(p, p_i) < d_E(p, p_j),\ j \neq i\} \tag{1}$$

i.e., a set of points in three-dimensional space R^3 which are closer to the nucleus point p_i than to any other nucleus points in S. In this sense, $v_E(p_i)$ is the dominant region of p_i. Each point in S generates its own v-cell; and all v-cells form a VD, which divides three-dimensional space into an array of convex, space-filling and non-overlapping polyhedrons with planar faces. The well-known PV diagram is a kind of VD with point set S generated through a homogeneous Poisson point process.

2.2. Voronoi diagram in Laguerre geometry

Voronoi diagram in Laguerre geometry (LV diagram), also referred to as power diagram, is a kind of weighted Voronoi diagram [12]. To point p_i in set S, a weight r_i is assigned, forming a weight set $r = \{r_1, r_2, \ldots, r_n\}$, and the distance between p_i and any point q is measured in Laguerre geometry

$$d_L(p_i, q) = \{[d_E(p_i, q)]^2 - r_i^2\}^{1/2} \tag{2}$$

Similar to VD, an lv-cell corresponding to point p_i is defined as

$$v_L(p_i) = \{p | p \in R^3,\ d_L(p, p_i) < d_L(p, p_j),\ j \neq i\} \tag{3}$$

and the set of all lv-cells, $V_L(S, r) = \{v_l(p_1), v_l(p_2), \ldots, v_l(p_n)\}$, is called an LV diagram. Here $v_l(p_i)$ is the dominant region of p_i with a weight of r_i. lv-Cells are also space-filling convex polyhedrons without overlapping interconnected in a topological manner in the same way as grains in polycrystalline materials.

2.3. Random closed packing of spheres (RCPS)

RCPS has been extensively studied by both experiments and computer simulations [13–16]. Computer algorithms used to generate RCPS can be classified into two catalogues: sequential generation method and collective rearrangement algorithms. In this paper a modified rearrangement algorithm is employed to generate RCPS [15,17] (Fig. 1).

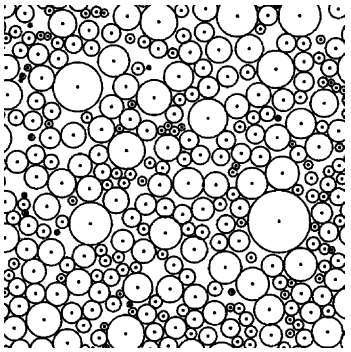

Fig. 1. A typical cross section of random closed packing of spheres, which have a lognormal volume distribution with CV = 2.0.

2.4. The RCP-LV diagram

The RCP-LV diagram is an LV diagram constructed based on RCPS, which provides point set S consisting of all the centers of spheres and weight set r of the corresponding radii (Fig. 2). In the RCP-LV diagram, each sphere has its own lv-cell, which, in return, encloses the whole sphere. Neighboring spheres belong to adjacent lv-cells. Tangent plane of two tangent spheres is just the sharing face of the corresponding polyhedrons. Thus, the volume distribution of lv-cells strongly inherits that of the original spheres. RCPS serves as a template in the generation of the RCP-LV diagram. In this paper, lv-cells are assumed to represent individual grains and RCP-LV diagram the microstructure of polycrystalline materials (Fig. 3).

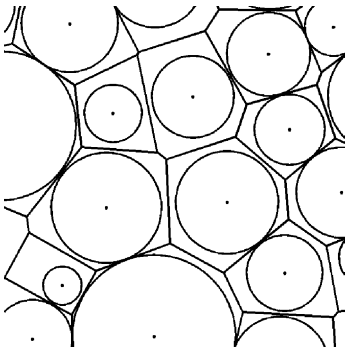

Fig. 2. A cross section of the RCP-LV diagram illustrating that RCPS serves as a template in the generation of the RCP-LV diagram.

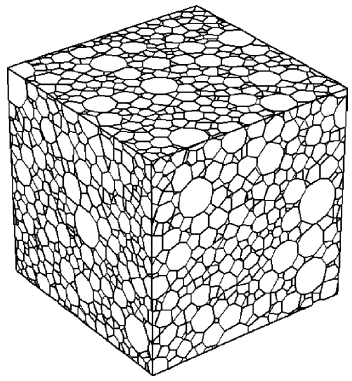

Fig. 3. Three cross sections of the RCP-LV diagram drawn based on random closed packing of spheres, which have a lognormal volume distribution with CV = 2.0.

2.5. Experimental procedure

In this paper, RCPS generation is done using collective rearrangement algorithm, whose details can be found in Refs. [15,17]; and RCP-LV diagram is drawn through four-dimensional convex hull constructed by the Qhull software package [18–20]. The experimental procedure is as follow:

1. We first generate random closed packing of 10,000 spheres within a cubic space. We keep the mean volume constant, i.e. unity, and the volume distribution lognormal with CV varying from 0.6 to 3.0 at intervals of 0.2, so 13 types of RCPS with different CV values are obtained.
2. We repeat this procedure for three times. In this way, for each type of RCPS, four groups of 10,000 spheres each are generated.
3. Each group of RCPS is transformed into an RCP-LV diagram.
4. To eliminate possible boundary effect, spheres centered within outermost shell of the initial cube two times the mean sphere diameters thick are not included in the further statistical procedure. As a result, each group of RCPS results in an RCP-LV diagram with about 5500 effective lv-cells.
5. For further analysis, we merge the four sets of statistical data of the RCP-LV diagrams drawn

based on RCPS with the same CV value into one.

6. Three-dimensional PV diagram with 96,000 v-cells (called pv-cells hereafter) is drawn using Qhull software package [18–20] to compare with our RCP-LV diagrams with various CV values.

3. Results and discussion

3.1. Volume and face number distributions

As the volume distribution in real material has been suggested to be lognormal by Rhines and Patterson [10] and Okazaki and Conrad [11], lognormal distribution is used to analyze our statistical data. Its probability density function is

$$f(x,\mu|\sigma) = \frac{1}{x\sigma\sqrt{2\pi}} \exp\left(\frac{-(\ln(x)-\mu)^2}{2\sigma^2}\right) \tag{4}$$

where μ and σ are two parameters related to expectation $E(x)$ and variance $\mathrm{Var}(x)$ by formulas

$$E(x) = \mathrm{e}^{(\mu+(\sigma^2/2))} \tag{5}$$

$$\mathrm{Var}(x) = \mathrm{e}^{(2\mu+2\sigma^2)} - \mathrm{e}^{(2\mu+\sigma^2)} \tag{6}$$

For comparison, we also introduce the gamma distribution, whose probability density function is

$$f(x,a|b) = \frac{1}{b^a\Gamma(a)} x^{a-1}\mathrm{e}^{-x/b} \tag{7}$$

where a and b are two parameters related to expectation $E(x)$ and variance $\mathrm{Var}(x)$ by formulas

$$E(x) = a \times b \tag{8}$$

$$\mathrm{Var}(x) = a \times b^2 \tag{9}$$

In formulas (5), (8) and (6), (9), $E(x)$ and $\mathrm{Var}(x)$ can be given by the unbiased estimators $\bar{x}$ and $\frac{1}{n-1}\sum_{i=1}^{n}(x_i-\bar{x})^2$, where x_i is the volume of the ith cell in certain diagram and $\bar{x}$ is the average of all the cell volumes in corresponding diagram. Now, we suppose the distributions of lv-cell volumes in RCP-LV diagrams and pv-cell volumes in PV diagram to be lognormal or gamma distribution, whose parameters are calculated using formulas (5) and (6) or formulas (8) and (9), respectively. Thereafter, we test these two hypotheses, using χ^2 goodness-of-fit test [21] (Figs. 4–6). Although the hypothesis that the distributions of lv-cell volumes in RCP-LV diagrams is gamma or lognormal at the significance level 0.05 is rejected, all the χ^2 of supposed lognormal distributions $\chi^2_{\log}$ are much

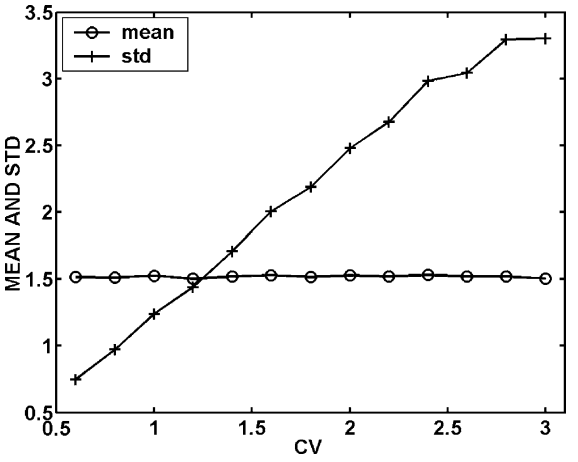

Fig. 4. The mean and standard deviation (std) of lv-cell volumes in the RCP-LV diagram vs. CV of sphere volumes in corresponding RCPS.

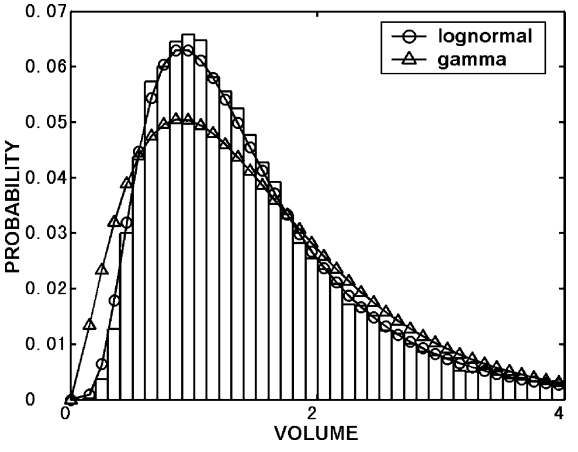

Fig. 5. The histogram of lv-cell volumes in the RCP-LV diagram and supposed gamma and lognormal distributions with corresponding parameters. This RCP-LV diagram is drawn based on RCPS, which have a lognormal volume distribution with CV = 0.8.

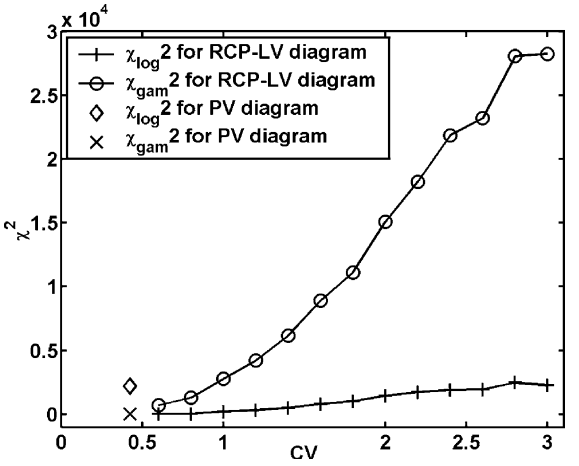

Fig. 6. The χ^2 values for volume distribution types test, in which the critical value $\chi^2_{0.05}$ is 14.067.

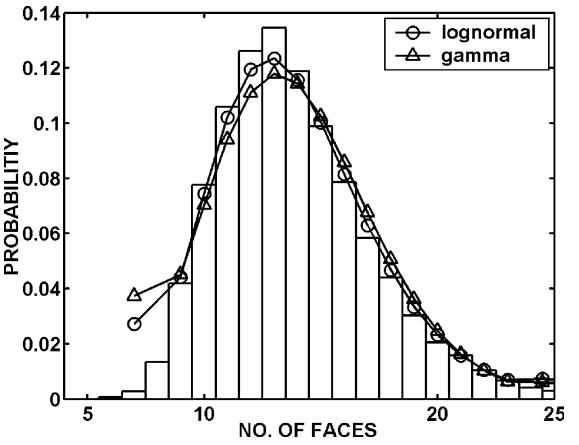

Fig. 7. The histogram of face number per lv-cell in the RCP-LV diagram and supposed gamma and lognormal distributions with corresponding parameters. This RCP-LV diagram is drawn based on RCPS, which have a lognormal volume distribution with CV = 0.8.

smaller than corresponding χ^2 of supposed gamma distributions χ^2_{gam}. On the other hand, although the hypothesis that the distributions of pv-cell volumes in PV diagram is gamma or lognormal at the significance level 0.05 is rejected, $\chi^2_{\log}$ is much larger than χ^2_{gam} in this case, which is consisted with the conclusion suggested by Kumar that pv-cell volumes approximately obey a gamma distribution in PV diagram [3]. So we can conclude that, lognormal distribution is a better approximation to the volume distribution in the present RCP-LV diagram than gamma distribution is; on the other hand, gamma distribution gives a better fit to volume distribution in PV diagram than lognormal distribution. The reason that volume distribution in the present RCP-LV diagram is more lognormal-like is that cell volume distribution is strongly influenced by that of spheres.

As the face number distribution in real material has also been suggested by Rhines and Patterson [10] to be lognormal, it is necessary to analyze the face number distribution in RCP-LV diagram and PV diagram by the same procedure as for volume distribution. Corresponding results are shown in Figs. 7 and 8. We also come to the same conclusion that the lognormal distribution is a better approximation to the face number distribution in the RCP-LV diagram than the gamma distribution; and the gamma distribution gives a better fit

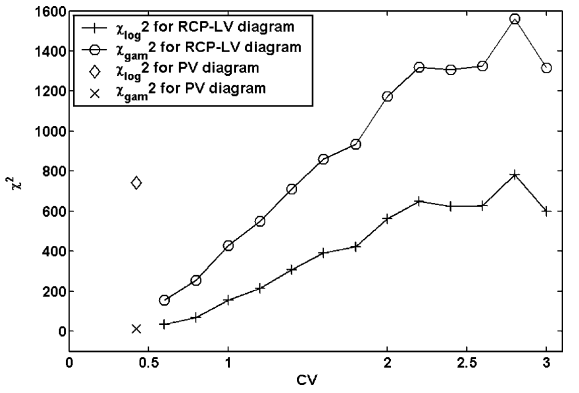

Fig. 8. The χ^2 values for face number distribution types test, in which the critical value $\chi^2_{0.05}$ is 14.067.

to face number distribution in the PV diagram than the lognormal distribution.

3.2. More analysis for RCP-LV diagram

For RCPS with certain CV value of sphere volumes, corresponding statistics, average number of faces per cell $\overline{F}$, average number of edges per face $\overline{E_F}$, and CV value of lv-cell volumes distribution CV_{cell}, are obtained. Fig. 9 shows the plot of $\overline{F}$ vs. CV of sphere volumes in corresponding

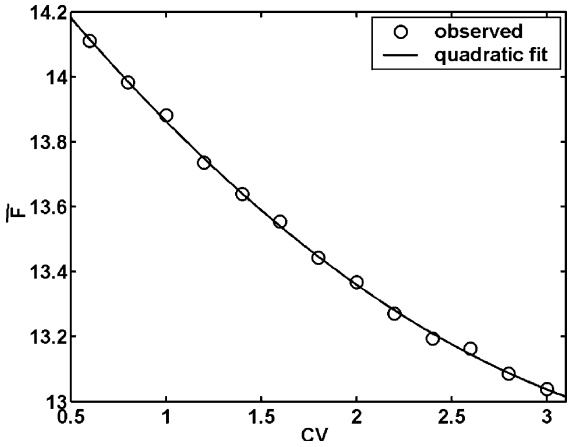

Fig. 9. The average number of faces per lv-cell in the RCP-LV diagram vs. CV of sphere volumes in corresponding RCPS.

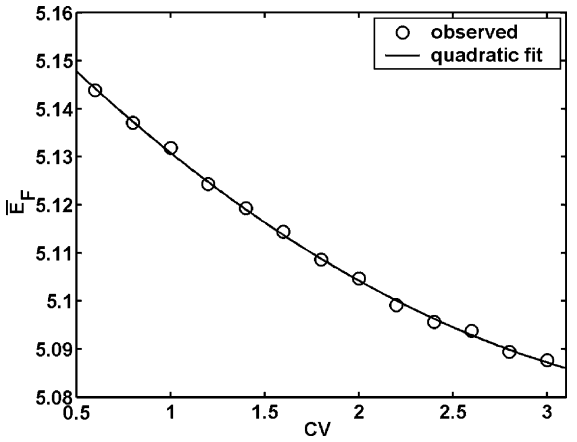

Fig. 10. The average number of edges per face in the RCP-LV diagram vs. CV of sphere volumes in corresponding RCPS.

RCPS. The relation between $\overline{E_F}$ and CV is drawn in Fig. 10, and the CV_{cell} vs. CV is shown in Fig. 11. Using a quadratic expression, $\overline{F}$ vs. CV and $\overline{E_F}$ vs. CV can be described as

$$\overline{F} = 0.09 \times (CV)^2 - 0.77 \times CV + 15 \quad (10)$$

with a norm of residuals of 0.038,

$$\overline{E_F} = 0.0048 \times (CV)^2 + 0.041 \times CV + 5.2 \quad (11)$$

with a norm of residuals of 0.0021.

We also fit a cubic expression to the relation of CV_{cell} vs. CV:

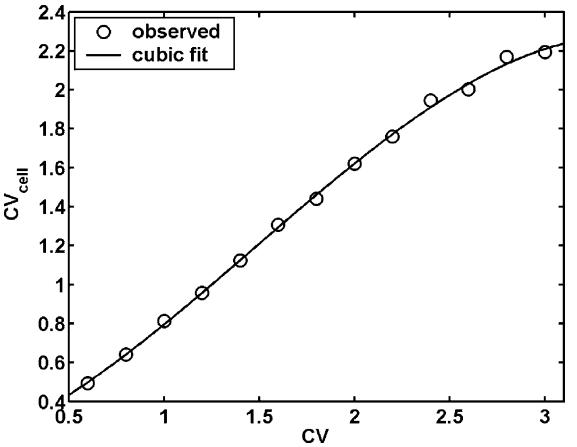

Fig. 11. CV of lv-cell volumes distribution in the RCP-LV diagram vs. CV of sphere volumes in corresponding RCPS.

$$CV_{cell} = -0.075 \times (CV)^3 + 0.33 \times (CV)^2 + 0.36 \times CV + 0.18 \quad (12)$$

with a norm of residuals of 0.068.

These figures show that when CV increases from 0.60 to 3.0, $\overline{F}$ decreases from 14.11 to 13.04, $\overline{E_F}$ from 5.14 to 5.09, while CV_{cell} increases from 0.49 to 2.19. It is worth mentioning here that, for most real materials, the average number of faces per grain $\overline{F}$, the average number of edges per face $\overline{E_F}$ and the CV values of grain volumes distribution are in these ranges (Table 1), while the corresponding statistic data in PV diagram are obviously far from these ranges. It is also shown clearly that CV_{cell} is controlled by CV of spheres in RCPS. This makes it easy to simulate polycrystalline microstructure with different CV values.

3.3. Simulation of grain growth

Rhines utilized three statistical parameters to measure width of properties' distributions while studying grains' growth [10]

$$\ln \sigma_E = \left[\frac{\sum_{i=1}^{m} \left(\ln E_i - \overline{\ln E} \right)^2}{m-1} \right]^{1/2} \quad (13)$$

$$\ln \sigma_F = \left[\frac{\sum_{i=1}^{n} \left(\ln F_i - \overline{\ln F} \right)^2}{n-1} \right]^{1/2} \quad (14)$$

Table 1
$\overline{F}$, $\overline{E}$ and CV of real materials

	No. of grains	$\overline{F}$	$\overline{E}$	CV	Ref.
β-brass	30	14.5	5.142	–	[4]
Aluminum–tin alloy	100	12.48	5.02 (5.06)	–	[5]
A steel	1215	13.184	–	–	[6]
A pure iron	–	13.42	–	–	[7]
Mixed bubbles	150	13.26	5.095	–	[8]
Uniform bubbles	600	13.702	5.111	–	[9]
Vegetable cells	450	13.802	5.123	–	[9]
Pure aluminum	92–349	–	–	1.09–2.13	[10]

$$\ln \sigma_V = \left[\frac{\sum_{i=1}^{n} \left(\ln V_i - \overline{\ln V} \right)^2}{n-1} \right]^{1/2} \tag{15}$$

where $\ln V_i$, $\ln F_i$ and $\ln E_i$ are the log of the volume of the ith grain, the log of the number of faces of the ith grain and the log of the number of edges of the ith face, respectively; and $\overline{\ln V}$, $\overline{\ln F}$, $\overline{\ln E}$ are their corresponding averages. He suggested that, in a real material, the relations of $\ln \sigma_E$ vs. $\ln \sigma_V$, $\ln \sigma_F$ vs. $\ln \sigma_V$, and the fraction of 3-edged faces vs. $\ln \sigma_E$ are all linear. These phenomena can also be found in the RCP-LV diagram (Figs. 12 and 13). Therefore, we may expect to use the RCP-LV diagram constructed based on RCPS with different CV values to simulate the statistical properties of grains in a real material under different grain growth stages.

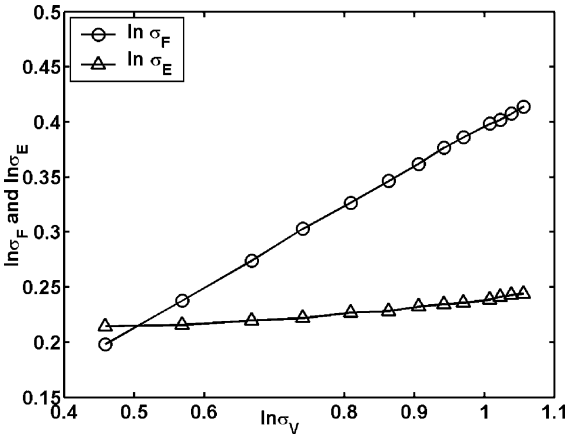

Fig. 12. The widths of the distributions of faces per cell and edges per face vs. the width of the cell volume distribution in the RCP-LV diagrams.

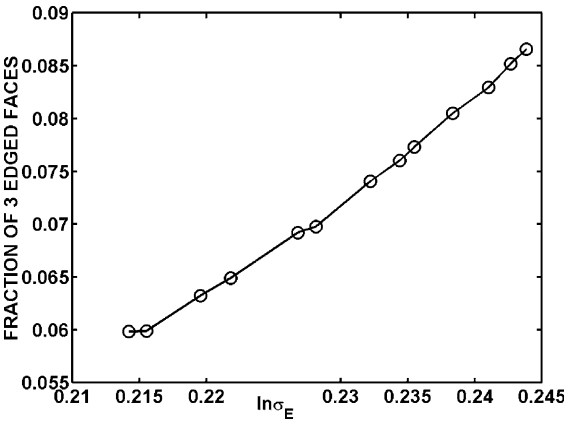

Fig. 13. The fraction of cell faces with three edges vs. the width of the distribution of edges per face in the RCP-LV diagrams.

3.4. Characteristics of the neighboring cells of an lv-cell

In materials science, a considerable interest is taken in the relationship between the value of a given characteristic for an individual grain and the mean value of that characteristic for contiguous grains. The most extensively studied characteristic is $\overline{F_F}$: The mean number of faces for the neighboring grains of an F-faced grain, which can be approximated by the function [22]

$$\overline{F_F} = A + B/F \tag{16}$$

We fit this function to the statistical data of 13 groups of RCP-LV diagrams based on RCPS with different CV values of sphere volumes; and, correspondingly, get 13 pairs of parameters A and B under those CV values (Figs. 14 and 15). From

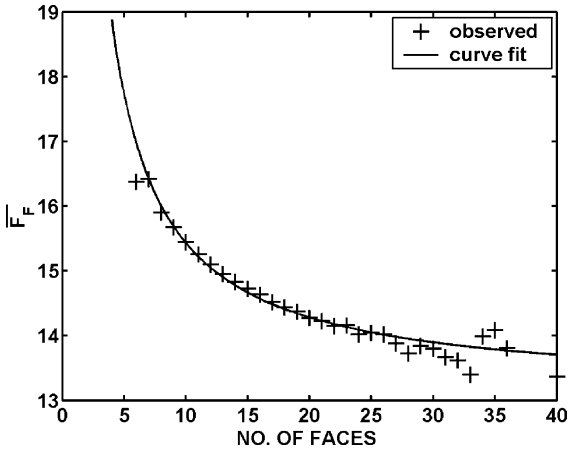

Fig. 14. $\overline{F_F}$ vs. number of faces per lv-cell in the RCP-LV diagram drawn based on RCPS, which have lognormal volume distribution with CV = 0.8.

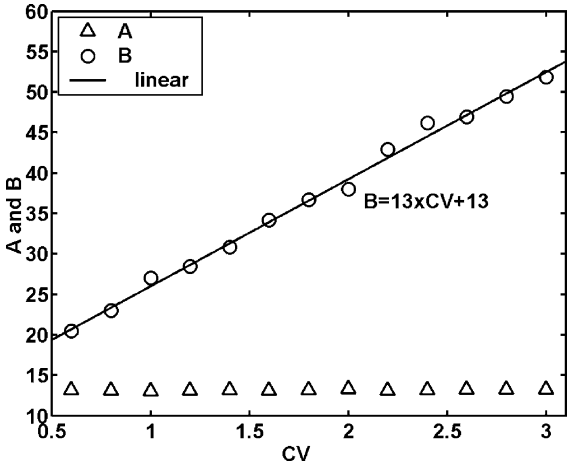

Fig. 15. The parameters A and B in function (14) vs. CV of sphere volumes in corresponding RCPS.

Fig. 15, we can learn that while the plot of A vs. CV oscillates in a narrow range, the plot of B vs. CV increases monotonously and approximately linearly.

4. Conclusion

We propose a model referred to as the RCP-LV diagram to simulate geometrical and topological characteristics in the microstructure of polycrystalline material. The distribution of lv-cell volumes in the RCP-LV diagram is strongly influenced by the lognormal distribution of sphere volumes in corresponding RCPS. In the RCP-LV diagram, statistical data, including volume and face number distributions, $\overline{F}$, $\overline{E}$ and CV_{cell} are much closer to those of a real material than in the PV diagram. Moreover, the relations of $\ln \sigma_E$ vs. $\ln \sigma_V$, $\ln \sigma_F$ vs. $\ln \sigma_V$, and the fraction of 3-edged faces vs. $\ln \sigma_E$ are consistent with the corresponding properties in the grain growth process for a real material. Hence, this model can also be used to reproduce structure evolution during grain growth.

References

[1] J.L. Meijering, Philllips Res. Rep. 8 (1953) 270.
[2] E.N. Gilbert, Annal. Math. Stat. 33 (1962) 958.
[3] S. Kumar, S.K. Kurtz, J.R. Banavar, M.G. Sharma, J. Stat. Phys. 67 (1992) 523.
[4] C.H. Desch, J. Inst. Met. 22 (1919) 241.
[5] W.M. Williams, C.S. Smith, Trans. Am. Inst. Min. Met. Eng. 194 (1952) 755.
[6] G. Liu, H. Yu, X. Qin, Mater. Sci. Eng. 326A (2002) 276.
[7] G. Liu, Thesis, University of Florida, 1984.
[8] E.B. Matzke, J. Nestler, Am. J. Botany 33 (1946) 130.
[9] E.B. Matzke, Am. J. Botany 33 (1946) 58.
[10] F.N. Rhines, B.R. Patterson, Metall. Trans. 13A (1982) 985.
[11] K. Okazaki, K. Conrad, Trans. Jpn. Inst. Met. 13 (1972) 198.
[12] F.A. Hemmer, ACM Comput. Surveys 23 (1991) 345.
[13] G.D. Scott, Nature 188 (1960) 908.
[14] G.D. Scott, D.M. Kilgour, J. Phys. D 2 (1969) 863.
[15] D. He, N.N. Ekere, J. Mater. Sci. Lett. 17 (1998) 1723.
[16] A.V. Galakhov, V.Ya. Shevchenko, Ceram. Inter. 18 (1992) 213.
[17] Y. Wu, Z. Fan, Y. Lu, J. Mater. Sci. 38 (2003) 2019.
[18] C.D. Barber, D.P. Dobkin, H.T. Huhdanpaa, The Quickhull algorithm for convex hulls, ACM Trans. Math. Softw. (December) (1996).
[19] K. Sugihara, Theor. Comput. Sci. 235 (2000) 325.
[20] Z. Fan, Y. Wu, X. Zhao, J. Tianjin University 36 (2003) 747.
[21] R.E. Walpole, R.H. Myers, Probability and Statistics for Engineers and Scientists, Prentice-Hall, Englewood Cliffs, NJ, 1993, p. 344.
[22] S.N. Chiu, Advances in Applied Probability 26 (1994) 565.